Exploration of Mechanisms Underlying the Strain-Rate-Dependent Mechanical Property of Single Chondrocytes

Trung Dung Nguyen, and YuanTong Gu [a)]

School of Chemistry, Physics and Mechanical Engineering, Queensland University of Technology, Brisbane, Queensland, Australia

Abstract – Based on the characterization by Atomic Force Microscopy (AFM), we report that the mechanical property of single chondrocytes has dependency on the strain-rates. By comparing the mechanical deformation responses and the Young's moduli of living and fixed chondrocytes at four different strain-rates, we explore the deformation mechanisms underlying this dependency property. We found that the strain-rate-dependent mechanical property of living cells is governed by both of the cellular cytoskeleton (CSK) and the intracellular fluid when the fixed chondrocytes is mainly governed by their intracellular fluid which is called the consolidation-dependent deformation behavior. Finally, we report that the porohyperelastic (PHE) constitutive material model which can capture the consolidation-dependent behavior of both living and fixed chondrocytes is a potential candidature to study living cell biomechanics.

Keywords **— Cell biomechanics, chondrocytes, AFM, strain-rate, Porohyperelastic (PHE) constitutive model.**

***<u>Corresponding author</u>*:**

Prof. YuanTong Gu

Address: School of Chemistry, Physics and Mechanical Engineering, Science and Engineering Faculty, Queensland University of Technology, 2 George Street, Brisbane, Queensland 4000, Australia

Phone: +61 7 3138 1009

Fax: +61 7 3138 1469

Email: yuantong.gu@qut.edu.au

Chondrocytes are cytoskeleton (CSK)-rich eukaryotic cells which are the mature cells in cartilage tissues performing a number of functions within the cartilage. Investigation of the mechanical properties and behaviors of chondrocytes plays an important role in understanding the cells' *in vivo* biomechanical environment. The alteration of the mechanical properties of these cells is believed to be one of the main factors in the development and progression of osteoarthritis [1, 2].

It is well-known that cells respond to their various mechanical environments that are caused by physiological conditions and diseases of which the cells are both the detectors and effectors. Physiological loads are usually applied at varying rates to achieve optimal biomechanical and biochemical outcomes in the body. Various studies have been conducted to investigate the effects of strain-rate on the mechanical responses of cartilages [3-5]. These studies concluded that strain-rate and magnitude of loading greatly influence chondrocyte death [6, 7], and that the response of tissue can be transformed from the fluid-dominate to purely elastic behavior by changing the rate of loading [4, 8]. However, little research has been conducted to investigate the strain-rate-dependent mechanical deformation properties of single chondrocytes. It is hypothesized that chondrocyte cells have similar strain-rate-dependent characteristics since Moeendarbary et al. stated that "the rate of cellular deformation is limited by the rate at which intracellular water can redistribute within the cytoplasm" [9]. The understanding of the strain-rate-dependent behavior of single cells is arguably a significant contribution that would provide insight into chondrocyte health in particular and cartilage dysfunction in general.

Because of recent advances in nanotechnology, a number of advanced experimental techniques for the direct characterization and study of the mechanical behaviors of single living cells have been developed. One such technique is based on Atomic Force Microscopy (AFM) which is a state-of-the-art experimental facility for high resolution imaging of tissues, cells and artificial surfaces, including probing the mechanical properties of samples both qualitatively and quantitatively [10-16]. Its principle is to indent the material/sample with a tip of microscopic dimension which is attached to a very flexible cantilever and the force is measured from the deflection of the cantilever to obtain the force-indentation (F-δ) curve [15, 17, 18]. This powerful tool is increasingly applied in the study of cell responses to external stimuli such as mechanical and chemical loading.

Thus, the aim of this study is to investigate the strain-rate-dependent mechanical properties of single chondrocytes using AFM. In order to explore the intracellular fluid predominant effect, the fixed chondrocytes were also investigated in this study since it is widely known that the CSK of fixed cells is stable [19] and thus is believed not respond to external mechanical stimuli as much as the intracellular fluid does. As a result, by comparing the strain-rate-dependent mechanical properties between living and fixed chondrocytes, it helps to shed an insight into the mechanisms underlying the dependency on the strain-rates behavior.

The chondrocytes were collected, cultured, and prepared before any AFM testing (supplemental material, section 1 [20]). AFM system used was a JPK NanoWizard II AFM (JPK Instruments, Germany). A triangular colloidal probe CP-PNPL-BSG-A-5 (NanoAndMore GMBH) cantilever was used in the experiment. The colloidal probe is of diameter around 5 μm and its spring constant was determined to be 0.0217 N/m using the thermal noise fluctuations before the indentation testing. Fig. 1(a) shows the Scanning Electron Microscope (SEM) image of the colloidal probe cantilever used. The colloidal probe was used because Dimitriadis et al. have proven that the smallest radius of the tip used in this study should be $R_{min} = 1.33\ \mu\mathrm{m}$ [21] so that the tip do not prompt local strains that exceed the material linearity regime. In addition, it was proven that spherical tipped cantilevers give more accurate results than sharp tipped cantilevers [21, 22]. Therefore, in this study we used the colloidal probe whose radius is around 2.5 μm which was also used widely for single cell mechanical testing [17, 18, 23]. The real diameter of the AFM bead, which is 5.44 μm, was measured using a Scanning Electron Microscope (SEM) (see Figure 1).

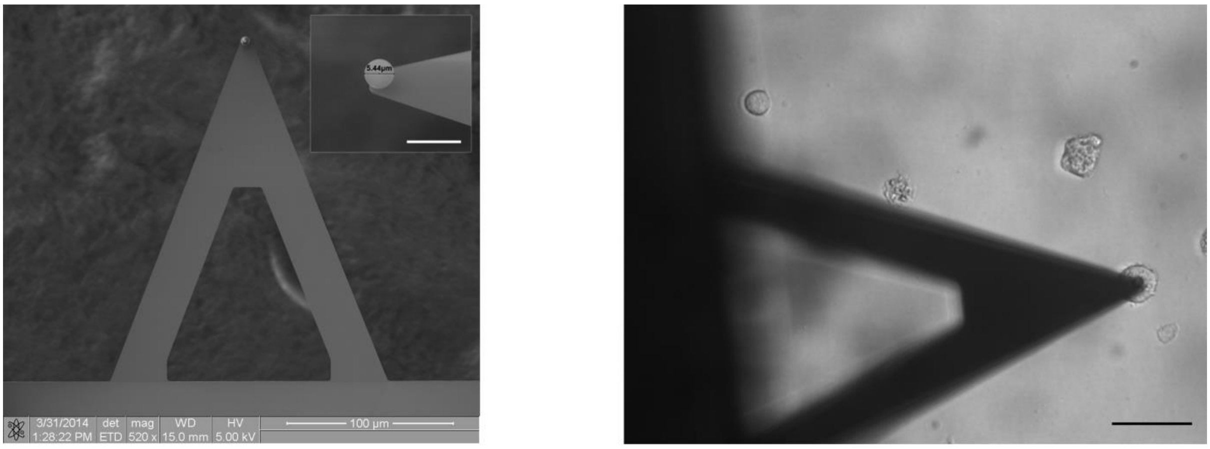

(a) (b)

Figure 1 (a) SEM image of colloidal probe cantilever used in this study (The inset shows the real diameter of the bead. Scale bar: 10 μm); (b) an indented living chondrocyte with a colloidal probe cantilever (Scale bar: 35 μm).

In our experiments, we firstly adjusted the position of the cantilever so that the colloidal probe lining up with the central (nuclear) region of the cell by using the Zeiss light microscope. Each single chondrocyte was then repeatedly indented 10 times (m = 10) at each of the four different strain-rates which are 2.92, 0.292, 0.0487, and 0.00487 s^{-1}. The indentation testing was conducted by controlling the absolute displacements of the piezoelectric scanner in Z-direction. Thus, the force set point threshold was not used in our study. In this study, we tested both living (n = 20) and fixed (n = 22) chondrocytes and the force-indentation curves were then obtained and preprocessed using JPKSPM data processing software version 4.4.23 (JPK Instruments, Germany) [24]. In order to investigate the strain-rate-dependent mechanical properties of chondrocytes, their Young's moduli at each of the four strain-rates were extracted from the force-indentation curves by using modified Hertzian model proposed by Dimitriadis et al. [21]. This model was developed for samples with finite thickness h which was measured based on a measurement technique to minimize the determination error (cell's height measurement procedure is shown in supplemental material [20]). Since colloidal probe cantilevers were used in our study, the relationship between the applied force F and indentation δ is:

$$F = \frac{4E}{3(1-\nu^2)} R^{1/2}\delta^{3/2}\left[1 - \frac{2\alpha_0}{\pi}\chi + \frac{4\alpha_0^2}{\pi^2}\chi^2 - \frac{8}{\pi^3}\left(\alpha_0^3 + \frac{4\pi^2}{15}\beta_0\right)\chi^3 + \frac{16\alpha_0}{\pi^4}\left(\alpha_0^3 + \frac{3\pi^2}{5}\beta_0\right)\chi^4\right] \quad (1)$$

where $\chi = \sqrt{R\delta}/h$, the constants α_0 and β_0 are functions of the material Poisson's ratio ν given below, E and R are Young's modulus and the radius of the rigid indenter e.g. 2.72 μm in this study, respectively. Because the cells have strong bond with the petri dish substrate, the constants α_0 and β_0 are given below [21]:

$$\alpha_0 = -\frac{1.2876 - 1.4678\nu + 1.3442\nu^2}{1-\nu} \quad (2)$$

$$\beta_0 = \frac{0.6387 - 1.0277\nu + 1.5164\nu^2}{1-\nu} \quad (3)$$

It is observed that there are two variables e.g. E and ν in the above equation. It was investigated that the measured properties changed by less than 20% when varying Poisson's ratio from 0.3 to 0.5 [25]. Thus for simplicity, the Poisson's ratio of chondrocytes was assumed to be 0.5 in this study [26]. As a result, the relationship between the applied force F and indentation δ becomes:

$$F = \frac{16E}{9} R^{1/2}\delta^{3/2}[1 + 1.133\chi + 1.283\chi^2 + 0.769\chi^3 + 0.0975\chi^4] \quad (4)$$

In order to determine the Young's moduli of chondrocytes, a program was developed using Matlab R2013a (The MathWorks, Inc.) based on the automatic AFM force curve analysis algorithm proposed by Lin et al .[27]

The behaviors of fixed chondrocytes were also studied and compared with that of living ones to study the effect of intracellular fluid. One-way analysis of variance (ANOVA) was employed using Minitab version 16.1.1 (Minitab Inc. 2010) with statistical significance reported at 95% confidence level ($p < 0.05$) between living and fixed chondrocytes at each of the four strain-rates.

Fig. 1(b) presents a typical indented living chondrocyte by a colloidal probe cantilever. Fig. 2(a) presents the force-indentation curves of a typical living and fixed chondrocytes. Also, Fig. 2 (b) and Table I show the average and standard deviation values of the Young's moduli for these cells. It is observed that both living and fixed cells have similar mechanical behaviors, in which the cells become more flexible with the decrease of strain-rates. Not surprisingly, this strain-rate-dependent deformation behaviors of chondrocytes are similar to the behaviors of articular cartilage tissue [4, 28].

Note that the Young's moduli of chondrocytes at low strain-rate determined in our study are consistent with published results [17, 25]. It is believed [4, 29] that the mechanisms underlying the strain-rate-dependent mechanical behavior were because of both the viscoelasticity of the cellular CSK and the intracellular fluid. Thus, in order to study only the effect of the intracellular fluid on mechanical behaviors of single cells, without loss of generality, fixed chondrocytes were used because it has been found [19] that the solid CSK of fixed cells is stable and thus does not play so important role as the intracellular fluid in the mechanical response to external loadings. Thus, by investigating the strain-rate-dependent mechanical properties of the fixed chondrocytes and comparing to living chondrocytes' ones, we can decouple the effect of viscoelasticity of the CSK.

Table I. Young's moduli (Pa) of living and fixed chondrocytes at four different strain-rates.

Strain-rates	0.00487 s^{-1}	0.0487 s^{-1}	0.292 s^{-1}	2.92 s^{-1}
Living chondrocytes (n = 20; m = 10)	470.13 ± 752.46	707.45 ± 569.09	784.84 ± 546.75	1370.73 ± 873.35
Fixed chondrocytes (n = 22; m = 10)	2298.9 ± 1388.97*	2420.38 ± 2219.85*	2731.83 ± 1639.62*	3642.7 ± 2140.62*

*$p < 0.001$ demonstrated that Young's moduli of fixed chondrocytes are significant larger than those of living chondrocytes at all strain-rates.

Fig. 2 (b) shows the average and standard deviation values of Young's moduli of living and fixed chondrocytes at four different strain-rates. It is observed that fixed chondrocytes are stiffer at the high strain-rate. It can be explained that at a high strain-rate the intracellular fluid does not move relative to the solid skeleton due to low permeability of the cell, as it is unable to escape quickly enough from the matrix and get trapped within the cell. It renders that the cell is almost incompressible because both fluid and solid constituents are incompressible. Therefore, the cell displays an almost classical elastic mechanical deformation response. In the other hand, the fixed chondrocytes were softer with decreasing of strain-rates corresponding to the reducing of Young's moduli (Fig. 2 (b)). This is because the intracellular fluid plays a dominate role and is able to exude from the cells matrix during indentation at these relative low strain-rates. Since the fluid was flown out from the cell, the chondrocyte underwent a net volume change and is therefore compressible. This is called the consolidation-dependent deformation behavior. It is interesting to note that the Young's modulus of fixed chondrocytes decreased dramatically with decreasing strain-rates of 2.92 to 0.0487 s^{-1} and reached an asymptotic/limiting value at 0.00487 s^{-1}. At such low strain-rate, the intracellular fluid can freely move through the solid CSK with very low resistance. Thus, it is believed that the strain-rate-dependent mechanical property of fixed chondrocytes is mainly governed by their intracellular fluid which plays an important role in cell biomechanics [9].

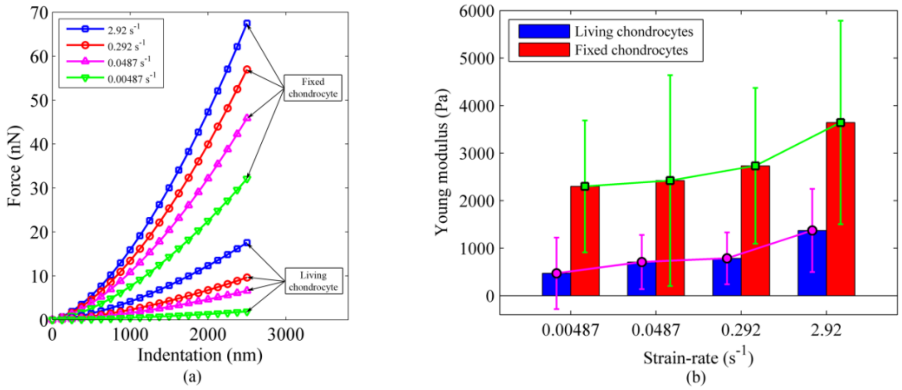

Figure 2 (a) Force-indentation curves corresponding to four different strain-rates of a typical living and fixed chondrocyte; (b) Young's moduli of living and fixed chondrocyte corresponding to four different strain-rates. Data are shown as mean ± standard deviation values.

From Fig. 2 (b), it can be clearly observed that living cells also had similar behavior, of which their stiffness reduced with decreasing of strain-rates (Fig. 2 (b) and Table I). However, the living cells were significantly softer than the fixed cells at all strain-rates ($p < 0.001$, Table I). It can be explained as the fixation process alters CSK's structure and properties [30, 31] which make the cells much stiffer than the living ones [18]. This is possible since Jungmann et al. also reported that the actin networks reflect the elasticity of the cells [32]. As observed in Fig. 2b, living chondrocytes' elastic moduli reduced almost linearly with decreasing of strain-rates without reaching a plateau value at 0.00487 s^{-1} compared to fixed chondrocytes. It is believed that it is because the cellular CSK reorganized or unbound its cross-linkers to respond to external loadings during deformations [33] which exhibits the important role of CSK especially at the low strain-rates. This is reasonable as Chahine et al. reported that there was no significant remodeling of actin and intermediate filaments observed during repetitive loading at the strain-rate within the intermediate range used in our study [34]. From the above discussions, it is concluded that both of the cellular CSK and intracellular fluid are important factors in controlling cellular mechanical behaviors, whereas only the CSK shows its predominant effect on the living cells at relatively low strain-rates.

As discussed above, both the CSK and intracellular fluid play important roles in the strain-rate-dependent mechanical behavior of the cells. In addition, it is widely known that the cell membrane is a porous and semi-permeable membrane gleaning certain substances to infiltrate the cell while keeping other substances out to protect the interior of the cell [35]. Thus, it is believed that the cytoplasm of the living cells behaves as a poroelastic material [9, 36], and also that of the fixed cells as observed in this study. This continuum model has been extended to include hyperelastic response of the non-linear solid skeleton leading to the porohyperelastic (PHE) material model (supplemental material, section 2 [20]). It considers the cell as consisting of an incompressible hyperelastic porous solid skeleton, saturated by an incompressible mobile fluid. This model which can account for the non-linear behaviors, fluid-solid interaction and rate-dependent drag effects is potentially a good candidate for investigating the responses of a cell to external loading and other load-inducing stimuli [37]. During attempting to apply PHE model in chondrocytes, we observed that both solid and fluid material parameters affected the performance of the model in simulating the strain-rate-dependent behavior. Thus, we believed that the PHE model can also be used to investigate the effect of both the CSK and the intracellular fluid in strain-rate-dependent mechanical deformation behavior of chondrocytes. In the same time this model has other advantages including that we can utilized all well-developed hyperelastic constitutive relationships such as Neo-Hookean, Mooney-Rivlin, Fung-Mooney, etc. and this constitutive law has been integrated in a commercial finite element software e.g. ABAQUS. Although the PHE model has been widely and effectively utilized in the tissue engineering at macroscale, e.g. the articular cartilage modelling [28, 38], and other poroelastic tissues [39-42], its application in the modelling of the single living cell is significantly limited.

To investigate the performance of the PHE model applying to single chondrocytes, the finite element analysis (FEA) models for living and fixed chondrocytes based on ABAQUS using the PHE model were developed (FEA model of chondrocytes and PHE material parameters determination procedure are shown in supplemental material [20]). Fig. 3 has proven that the PHE model can capture the consolidation-dependent behavior of both living and fixed chondrocytes. We can conclude that the PHE constitutive model is a promising constitutive model to simulate the strain-rate-dependent property as well as other behaviors of single cells, although we will conduct studies for numerical modelling of other types of cells in our future work.

In summary, this study investigated the strain-rate-dependent mechanical property of living and fixed chondrocytes using AFM. The results revealed that both living and fixed cells have similar mechanical deformation behavior, of which their stiffness reduced with decreasing of strain-rates, and that both CSK and the intracellular fluid governed the strain-rate-dependent property of living cells when the fixed chondrocytes' behavior is mainly governed by their intracellular fluid which is called consolidation-dependent deformation behavior. Finally, the porohyperelastic (PHE) constitutive model is developed based on the experimental results. It has been found that the PHE model can capture the consolidation-dependent behavior of both living and fixed chondrocytes. Therefore, we report that the PHE model is a suitable mechanical constitutive model for cell biomechanics.

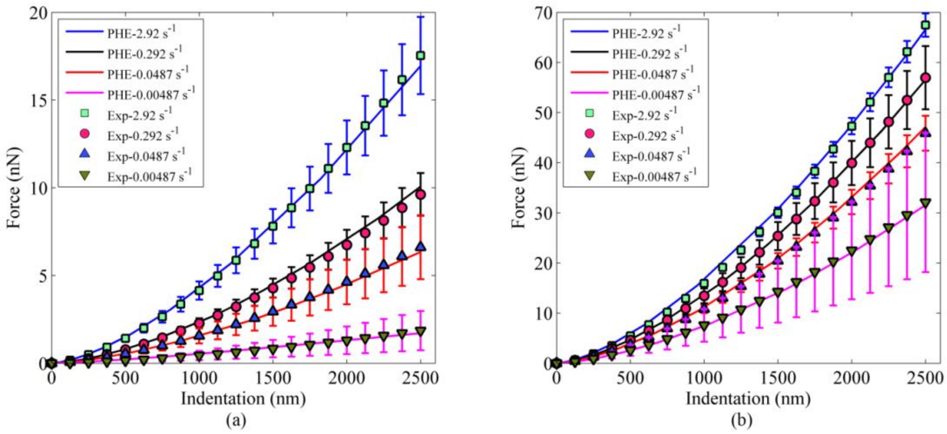

Figure 3 Experimental and PHE force-indentation curves of a typical (a) living and (b) fixed chondrocyte at four different strain-rates.

This research was funded by ARC Future Fellowship project (FT100100172) and QUT Postgraduate Research Scholarship. This work was performed in part at the Queensland node of the Australian National Fabrication Facility (ANFF), a company established under the National Collaborative Research Infrastructure Strategy to provide nano and micro-fabrication facilities for Australia's researchers. The authors gratefully acknowledge Dr. Sanjleena Singh for primary chondrocytes supply and also experimental assistance. The authors would also thank Mr. Tong Li for his suggestions to improve the paper’s quality and Mr. Arixin Bo for his SEM experimental assistance.

REFERENCES

1. W. R. Jones, H. P. Ting-Beall, G. M. Lee, S. S. Kelley, R. M. Hochmuth and F. Guilak, in *43rd Annual Meeting, Orthopaedic Research Society* (San Francisco, California, 1997).
2. W. R. Trickey, G. M. Lee and F. Guilak, Journal of Orthopaedic Research **18**, 891-898 (2000).
3. E. K. Moo, W. Herzog, S. K. Han, N. A. Abu Osman, B. Pingguan-Murphy and S. Federico, Biomech Model Mechanobiol **11**, 983-993 (2012).
4. A. Oloyede, R. Flachsmann and N. D. Broom, Connective Tissue Research **27**, 211-224 (1992).
5. T. M. Quinn, R. G. Allen, B. J. Schalet, P. Perumbuli and E. B. Hunziker, Journal of Orthopaedic Research **19**, 242-249 (2001).
6. B. Kurz, M. Jin, P. Patwari, D. M. Cheng, M. W. Lark and A. J. Grodzinsky, Journal of Orthopaedic Research **19**, 1140-1146 (2001).
7. B. J. Ewers, D. Dvoracek-Driksna, M. W. Orth and R. C. Haut, Journal of Orthopaedic Research **19**, 779-784 (2001).
8. A. Oloyede and N. Broom, Connective tissue research **30** (2), 127 (1993).
9. E. Moeendarbary, L. Valon, M. Fritzsche, A. R. Harris, D. A. Moulding, A. J. Thrasher, E. Stride, L. Mahadevan and G. T. Charras, Nature materials **12** (3), 253-261 (2013).
10. A. Touhami, B. Nysten and Y. F. Dufrene, Langmuir **19**, 4539-4543 (2003).
11. F. Rico, P. Roca-Cusachs, N. Gavara, R. Farre, M. Rotger and D. Navajas, Physical Review **72** (021914), 1-10 (2005).
12. C. Y. Zhang and Y. W. Zhang, Philosophical Magazine **87** (23), 3415-3435 (2007).
13. D. C. Lin, E. K. Dimitriadis and F. Horkay, eXPRESS Polymer Letters **1** (9), 576-584 (2007).
14. T. G. Kuznetsova, M. N. Starodubtseva, N. I. Yegorenkov, S. A. Chizhik and R. I. Zhanov, Micron **38**, 824-833 (2007).
15. E. C. Faria, N. Ma, E. Gazi, P. Gardner, M. Brown, N. W. Clarke and R. D. Snook, Analyst **133**, 1498-1500 (2008).
16. K. Q. Yusuf, N. Motta, Z. Pawlak and A. Oloyede, Connective Tissue Research **53** (3), 236-245 (2012).
17. E. M. Darling, S. Zauscher and F. Guilak, Osteoarthritis and Cartilage **14**, 571-579 (2006).
18. H. Ladjal, J. L. Hanus, A. Pillarisetti, C. Keefer, A. Ferreira and J. P. Desai, in *IEEE/RSJ International Conference on Intelligent Robots and Systems* (St. Louis, MO: Univted States, 2009).
19. T. Svitkina, in *Cytoskeleton Methods and Protocols* (Springer, 2010), pp. 187-206.
20. See supplementary material at [URL will be inserted by AIP] for more information about PHE theory, sample preparation, and cell's height measurement procedure.
21. E. K. Dimitriadis, F. Horkay, J. Maresca, B. Kachar and R. S. Chadwick, Biophysical Journal **82**, 2798-2810 (2002).
22. A. R. Harris and G. T. Charras, Nanotechnology **22** (34), 345102 (2011).
23. Q. S. Li, G. Y. H. Lee, C. N. Ong and C. T. Lim, Biochemical and Biophysical Research Communications **374**, 609-613 (2008).
24. JPK-Instruments, (JPK Instruments, 2011).
25. E. M. Darling, M. Topel, S. Zauscher, T. P. Vail and F. Guilak, Journal of biomechanics **41** (2), 454-464 (2008).
26. E. H. Zhou, C. T. Lim and S. T. Quek, Mechanics of Advanced Materials and Structures **12** (6), 501-512 (2005).
27. D. C. Lin, E. K. Dimitriadis and F. Horkay, Journal of biomechanical engineering **129** (3), 430-440 (2007).
28. A. Oloyede and N. D. Broom, Clinical Biomechanics **6** (4), 206–212 (1991).
29. W. R. Trickey, F. P. T. Baaijens, T. A. Laursen, L. G. Alexopoulos and F. Guilak, Journal of Biomechanics **39** (1), 78-87 (2006).
30. Y. Yamane, H. Shiga, H. Haga, K. Kawabata, K. Abe and E. Ito, Journal of electron microscopy **49** (3), 463-471 (2000).
31. A. G. Vegh, C. Fazakas, K. Nagy, I. Wilhelm, I. A. Krizbai, P. Nagyőszi, Z. Szegletes and G. Váró, Journal of Molecular Recognition **24** (3), 422-428 (2011).
32. P. M. Jungmann, A. T. Mehlhorn, H. Schmal, H. Schillers, H. Oberleithner and N. P. Südkamp, Tissue Engineering Part A **18** (9-10), 1035-1044 (2012).
33. O. Lieleg, J. Kayser, G. Brambilla, L. Cipelletti and A. R. Bausch, Nature materials **10** (3), 236-242 (2011).
34. N. O. Chahine, C. Blanchette, C. B. Thomas, J. Lu, D. Haudenschild and G. G. Loots, PloS one **8** (4), e61651 (2013).
35. P. L. Yeagle, The FASEB journal **3** (7), 1833-1842 (1989).
36. E. H. Zhou, F. D. Martinez and J. J. Fredberg, Nature materials **12** (3), 184-185 (2013).
37. T. D. NGUYEN, Y. T. GU, A. OLOYEDE and W. SENADEERA, International Journal of Computational Methods **11** (No. Suppl. 1), 1-20 (2014).

38. A. Oloyede and N. D. Broom, Connective Tissue Research **34** (2), 119-143 (1996).
39. M. V. Kaufmann, The University of Arizona, Tucson, AZ, 1996.
40. B. R. Simon, M. V. Kaufmann, M. A. McAfee and A. L. Baldwin, ASME Journal of Biomechanical Engineering **120**, 296-298 (1998).
41. P. H. Rigby, R. I. Park and B. R. Simon, 2004 (unpublished).
42. A. Ayyalasomayajula, J. P. Vande Geest and B. R. Simon, Journal of biomechanical engineering **132** (10) (2010).